Journal of Magnetism and Magnetic Materials 412 (2016) 1–6

Contents lists available at ScienceDirect

Journal of Magnetism and Magnetic Materials

journal homepage: www.elsevier.com/locate/jmmm

Nomograph method for predicting magnetoelectric coupling

Mirza Bichurin*, Vladimir Petrov, Roman Petrov, Alexander Tatarenko, Viktor Leontiev, Ksenia Lavrentieva

Institute of Electronic and Information Systems, Novgorod State University, 41 B.S.-Peterburgskaya Street, 173003 Veliky Novgorod, Russia

ARTICLE INFO

Article history:
Received 5 November 2015
Received in revised form
11 March 2016
Accepted 22 March 2016
Available online 24 March 2016

Keywords:
Magnetoelectric coupling
Magnetically induced ME effect
Magnetostrictive material
Composite materials

ABSTRACT

Magnetoelectric (ME) composites are known to enable the achievement of ME voltage coefficients many orders of magnitude larger than previously reported values for single phase materials. The advancements have opened up many possibilities in applications of sensors, transformers, and microwave devices. We presented here a new quick test of ME composites using nomographs and showed its use in applications where an approximate answer is appropriate and useful. To draw the graphs for ME voltage coefficients, we derived approximate expressions in explicit form for magnetically induced ME effect for different operational modes and laminate composite configurations including symmetrical and asymmetrical structures.

1. Introduction

Magnetoelectric (ME) interactions in magnetostrictive-piezoelectric multiferroic structures are intensively studied in recent years for their applications in magnetic field sensors, transducers and energy harvesters [1–11]. ME interaction exhibits itself as inducing the electric field E across the structure in an applied ac magnetic field H and arises as a product property of magnetostriction in magnetic layer and piezoelectricity in piezoelectric layer. ME coupling strength is characterized by the ME voltage coefficient $\alpha_E = E/H$. It is the practice to obtain the estimates of magnetoelectric (ME) voltage coefficients by solving the set of analytic equations. However, it's a difficult problem. Estimates of ME coupling strength can be obtained by using the numerical graphical database presented recently for several compositions for low-frequency [12] and magnetic resonance [13] regions. A model was recently proposed to optimize the design of magnetoelectric composites for low frequency sensor application [14]. The influence of the properties of piezoelectric and piezomagnetic materials, volume fraction, and magnetic field orientation on the induced voltage were evaluated. We suggest using the nomograph method that facilitates the efficient estimates of ME coefficients from given parameters of composite components. To draw the graphs for ME voltage coefficients, we obtained approximate expressions for magnetically induced ME effect in explicit form for different operational modes and laminate composite configurations including symmetrical and asymmetrical (bilayer) structures. Results from a nomogram can be obtained very quickly and reliably. In addition, nomograms are known to naturally incorporate the domain knowledge into their design. It should be noted that the nomogram's accuracy is limited by the precision of reproducing the physical parameters. Most nomograms are used in applications where an approximate answer is appropriate and useful. On the other hand, a nomogram may be used to verify an estimate obtained from another exact calculation method. Thus a nomogram is designed to perform a specific calculation.

In ME composites, the induced polarization P is related to the magnetic field H by the expression, $P = \alpha H$, where α is the second rank ME-susceptibility tensor. The (static) effect was first observed in antiferromagnetic Cr_2O_3. The ME effect was first observed in single crystals [15] of single phase materials a little more 50 years ago, and subsequently in polycrystalline single phase materials. The largest value of a ME for a single phase material is that for Cr_2O_3 crystals [16], where $a_{ME} = 20$ mV/cm-Oe. In last few years, strong magneto-elastic and elasto-electric coupling has been achieved through optimization of material properties and proper design of transducer structures. Lead zirconate titanate (PZT)-ferrite, PZT-Terfenol-D and PZT-Metglas are the most studied composites to-date. One of largest ME voltage coefficient of 500 Vcm-1 Oe-1 was reported recently for a high permeability magnetostrictive piezofiber laminate [17]. These developments have led to ME structures that provide high sensitivity over a varying range of frequency and DC bias fields enabling the possibility of practical applications [18].

In order to obtain high ME couplings, a layered structure must be insulating, in order that it can be poled to align the electric dipole moments. The poling procedure involved heating the sample to 420 K, and re-cooling to 300 K under an electric field of

* Corresponding author.
E-mail address: mirza.bichurin@novsu.ru (M. Bichurin).

http://dx.doi.org/10.1016/j.jmmm.2016.03.070
0304-8853/

E=20–50 kV/cm. The samples are then placed between the pole pieces of an electromagnet (0–18 kOe) used for applying a magnetic bias field H. The required AC magnetic field δH=1 Oe at 10 Hz to 100 kHz applied parallel to H is generated with a pair of Helmholtz coils. The AC electric field δE perpendicular to the sample plane is estimated from the measured voltage δV. The ME coefficient a_E is measured for three conditions: (1) transverse or $a_{E,31}$ for H and δH parallel to each other and to the disk plane (1,2) and perpendicular to δE (direction-3), (2) longitudinal or $a_{E,33}$ for all the three fields parallel to each other and perpendicular to sample plane and (3) in-plane $a_{E,11}$ for all the three fields parallel to each other and parallel to sample plane. An ME phenomenon of fundamental and technological interests is an enhancement in the coupling, when the electrical or magnetic sub-system undergoes resonance: i.e., electromechanical resonance (EMR) for PZT and ferromagnetic resonance (FMR) for the ferrite. As the dynamic magnetostriction is responsible for the electromagnetic coupling, EMR leads to significant increasing in the ME voltage coefficients. In case of resonance ME effects at FMR an electric field E produces a mechanical deformation in the piezoelectric phase, resulting in a shift in the resonance field for the ferromagnet. Besides, the peak ME voltage coefficient occurs at the merging point of acoustic resonance and FMR frequencies, i.e., at the magnetoacoustic resonance [19]. Then we discuss the estimations of ME effects in the different frequency ranges.

2. Low-frequency magnetoelectric coupling

We consider more often used in practice the transverse fields' orientation that corresponds to E and δE being applied along the X_3 direction, and H and δH along the X_1 direction (in the sample plane). The expression for the transverse ME voltage coefficient is [12]

$$\alpha_{E,31} = \frac{E_3}{H_1} = \frac{-V(1-V)({}^m q_{11} + {}^m q_{21}){}^p d_{31}}{{}^p\epsilon_{33}({}^m s_{12} + {}^m s_{11})v + {}^p\epsilon_{33}({}^p s_{11} + {}^p s_{12})(1-V) - 2\,{}^p d_{31}^2(1-V)}. \quad (1)$$

For symmetric trilayer structures, using the 1-D approximations, the expression for transverse ME voltage coefficient takes on the form:

$$\alpha_{E,31} = \frac{V(1-V)x}{\epsilon_0[{}^m s_{11}V + {}^p s_{11}(1-V)]} \quad (2)$$

where $x = {}^m q_{11}\frac{{}^p d_{31}}{{}^p\varepsilon_{33}/\varepsilon_0}$, , ${}^p s_{11}$, ${}^m s_{11}$, ${}^p d_{31}$ and ${}^m q_{11}$ are compliance, and piezoelectric and piezomagnetic coupling coefficients for piezoelectric and piezomagnetic layers, respectively, ${}^p\varepsilon_{33}$ is the permittivity of piezoelectric layer. In Eq. (2), the electromechanical coupling factor is assumed to satisfy the condition: ${}^pK_{31}^2 = {}^p d_{31}^2/{}^p s_{11}{}^p\varepsilon_{33} << 1$.

For convenience we suggest using the nomograph method to estimate the ME voltage coefficients from given parameters of composite components.

Figs. 1 and 2 present the ME voltage coefficients as a function of piezoelectric volume fraction. As an example, estimates are obtained for transverse fields' orientation (in-plane ac and dc magnetic fields and out-of-plane ac electric field and poling direction). However, ME voltage coefficients for longitudinal (out-of-plane electric and magnetic fields) and in-plane longitudinal fields orientations can be easily obtained by replacing the piezomagnetic coefficient q_{11} in Eq. (2) with q_{31} for longitudinal and replacing the piezoelectric coefficient d_{31} in Eq. (2) with d_{33} for in-plane longitudinal fields' orientation. The theory predicts the highest ME coupling for in-plane fields.

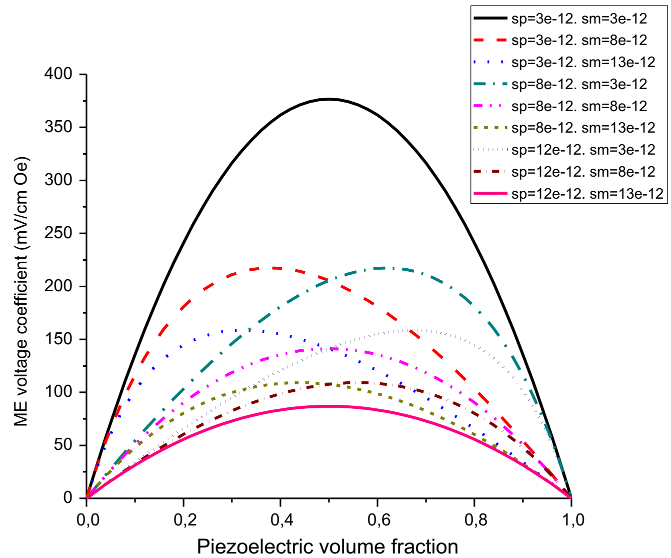

Fig. 1. Piezoelectric volume fraction dependence of transverse ME voltage coellicient for simmetric layered structure of magnetoctrictive and piezoelectric components with different compliencecs for x=0.5 · 10^{-22} (in SI units).

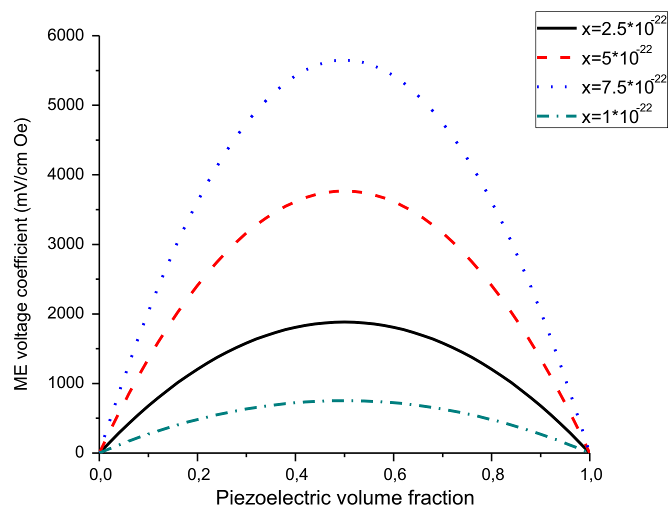

Fig. 2. Piezoelectric volume fraction dependence of transverse ME voltage coellicient for simmetric layered structure of magnetoctrictive and piezoelectric components for different x-values.

For the bilayer structure, the ME voltage coefficient should be calculated taking into account the flexural deformations. On the foregoing assumptions, our model enables deriving the explicit expression for ME voltage coefficient:

$$\frac{\delta E_3}{\delta H_1} = \frac{[1^p s_{11} + {}^m s_{11} r^3]\,{}^m q_{11}{}^p d_{31}/{}^p\varepsilon_{33}}{{}^p s_{11}[2r^m s_{11}(2+3r+2r^2) + {}^p s_{11}] + {}^m s_{11}^2 r^4}. \quad (3)$$

where $r={}^pt/{}^mt$ with ${}^pt$ and ${}^mt$ denoting the thickness of piezoelectric and magnetostrictive layer, correspondingly.

Eq. (3) is written in a simplified form under assumption ${}^pK_{31}^2 << 1$ similarly to deriving Eq. (2).

Piezoelectric volume dependence of ME voltage coefficient reveals a double maximum that is due to fact that the strain produced by the magnetic component consists of two components: longitudinal and flexural. In the absence of flexural strain the maximum ME coefficient occurs for certain value of volume fraction [12]. Since the flexural strain is of opposite sign relative to

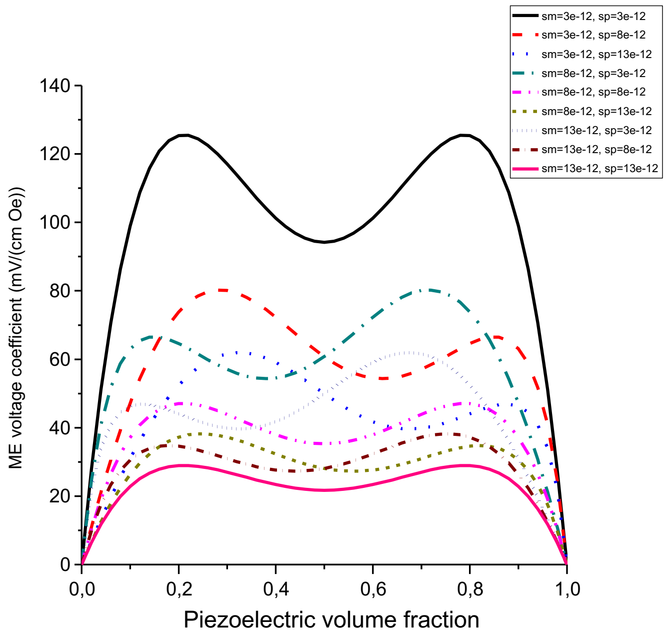

Fig. 3. Piezoelectric volume fraction dependence of transverse ME voltage coellicient for bilayer of magnetoctrictive and piezoelectric components with different compliencecs for $x=0.5\cdot10^{-22}$ (in SI units).

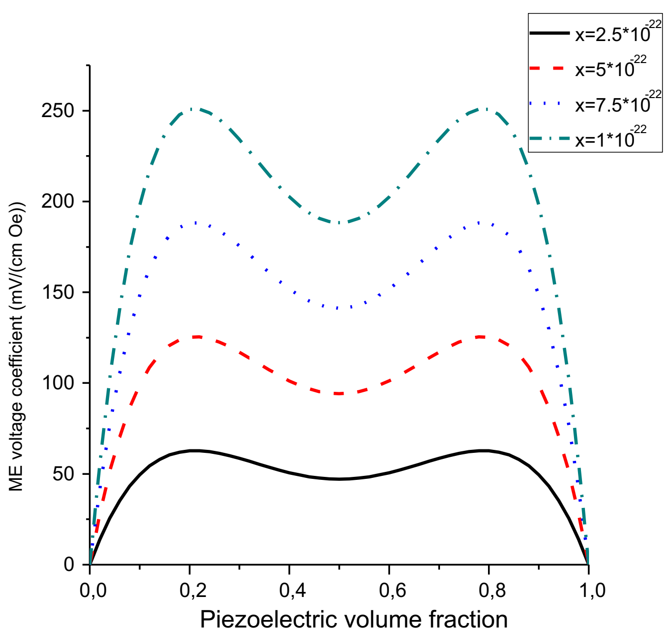

Fig. 4. Piezoelectric volume fraction dependence of transverse ME voltage coellicient for bilayer of magnetoctrictive and piezoelectric components at different x values in SI units.

longitudinal strain and reaches its maximum value approximately for the same volume fraction, the two types of strains combine to produce suppression of $\alpha_{E,31}$ in the middle and a double maximum in the ME coefficient piezoelectric volume dependence of ME voltage coefficient as in Figs. 3 and 4.

3. Magnetoelectric coupling at bending mode

Next we consider ME coupling under small-amplitude flexural oscillations of a bilayer rigidly clamped at one end. The bilayer

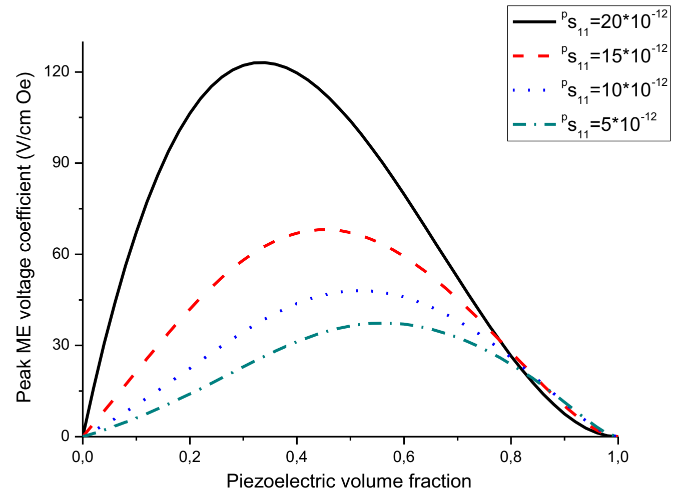

Fig. 5. Piezoelectric volume fraction dependence of peak ME voltage coefficient at bending mode of magnetostrictive-piezoelectric bilayer for ${}^{m}s_{11}=5\cdot10^{-12}$ m^2/N and different values of ${}^{p}s_{11}$. Value of x_1 is assumed to be equal to $5\cdot10^{-20}$ (in SI units).

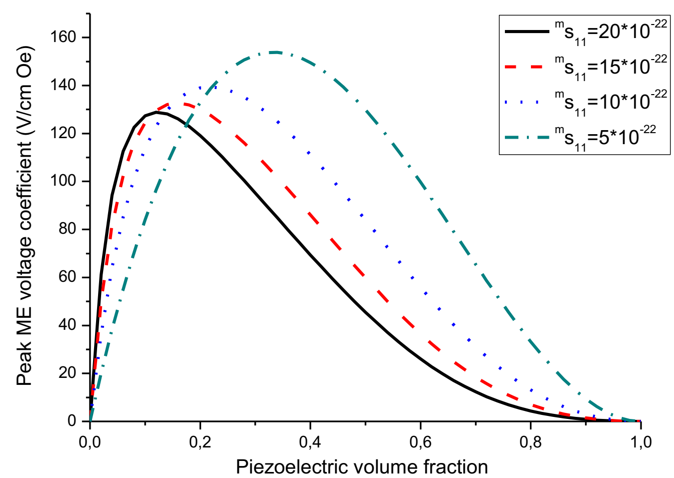

Fig. 6. Piezoelectric volume fraction dependence of peak ME voltage coefficient at bending mode of magnetostrictive-piezoelectric bilayer for ${}^{p}s_{11}=5\cdot10^{-12}$ m^2/N and different values of ${}^{m}s_{11}$. Value of x_1 is assumed to be equal to $5\cdot10^{-20}$ (in SI units).

deflection should obey the equations of bending motion provided in our models in Ref. [11]. To solve these equations, we used the boundary conditions that the bilayer deflection and its derivative vanish at clamped end of the bilayer and rotational moment and transverse force vanish at free end. Under assumption ${}^{p}K_{31}^{2}<<1$ and ${}^{m}K_{11}^{2}<<1$ (${}^{m}K_{11}^{2}={}^{m}q_{11}^{2}/({}^{m}s_{11}{}^{m}\mu_{11})$ with ${}^{m}\mu_{11}$ denoting the absolute permeability of magnetic layer), the resonance condition is $\cosh(kL)\cdot\cos(kL)=-1$ with k being the wave number.

The ME voltage coefficient at bending mode frequency can be estimated as

$$\frac{\delta E_3}{\delta H_1}=\frac{0.0766Q_b{}^{m}t({}^{m}t+2z_0)(2z_0-{}^{p}t){}^{p}d_{31}{}^{m}q_{11}}{D{}^{p}s_{11}{}^{m}s_{11}{}^{p}\varepsilon_{33}} \tag{4}$$

where D and Q_a are cylindrical stiffness sample and the quality factor for the bending resonance. The peak ME voltage coefficient is dictated by Q value, piezoelectric and piezomagnetic coupling coefficients, elastic compliances and volume fractions of initial components. Eq. (4) can be put in a more convenient form $\alpha_{E,\,31}=\frac{0.0766{}^{m}t({}^{m}t+2z_0)(2z_0-{}^{p}t)x_1}{D{}^{p}s_{11}{}^{m}s_{11}\varepsilon_0}$ where $x_1=\frac{{}^{p}d_{31}{}^{m}q_{11}Q_b}{{}^{p}\varepsilon_{33}/\varepsilon_0}$. Piezoelectric

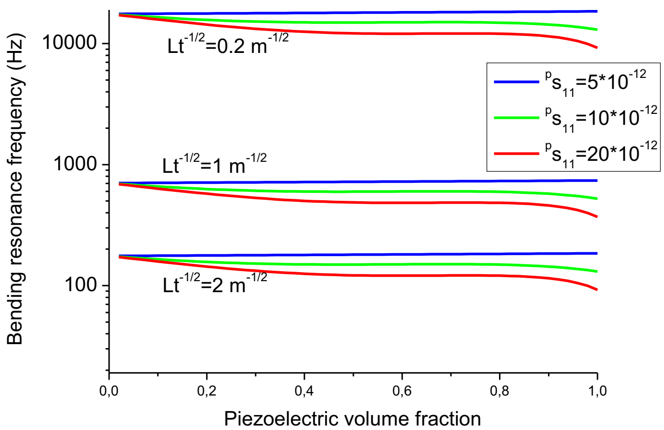

Fig. 7. Piezoelectric volume fraction dependence of bending resonance frequency of magnetostrictive-piezoelectric bilayer for ${}^{m}s_{11}=5\cdot10^{-12}$ m^2/N and different values of ${}^{p}s_{11}$ and Lt$^{-½}$.

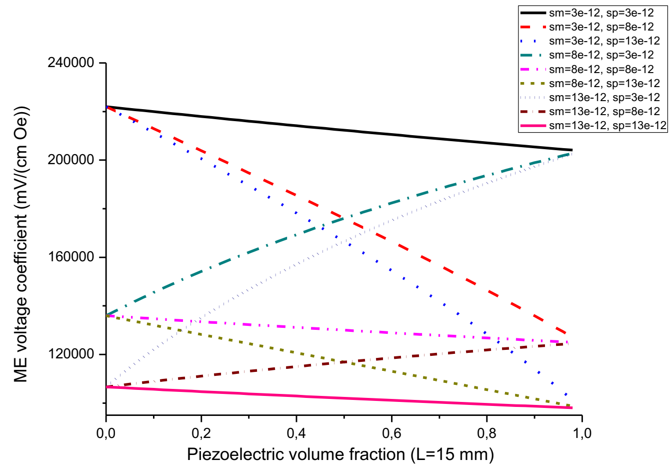

Fig. 10. EMR frequency versus piezoelectric volume fraction for longitudinal mode of 15 mm long magnetostrictive-piezoelectric layered structure.

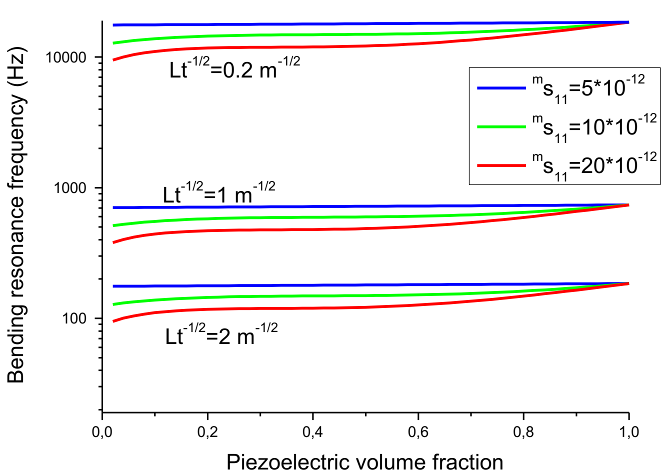

Fig. 8. Piezoelectric volume fraction dependence of bending resonance frequency of magnetostrictive-piezoelectric bilayer for ${}^{p}s_{11}=5\cdot10^{-12}$ m^2/N and different values of ${}^{m}s_{11}$ and Lt$^{-½}$.

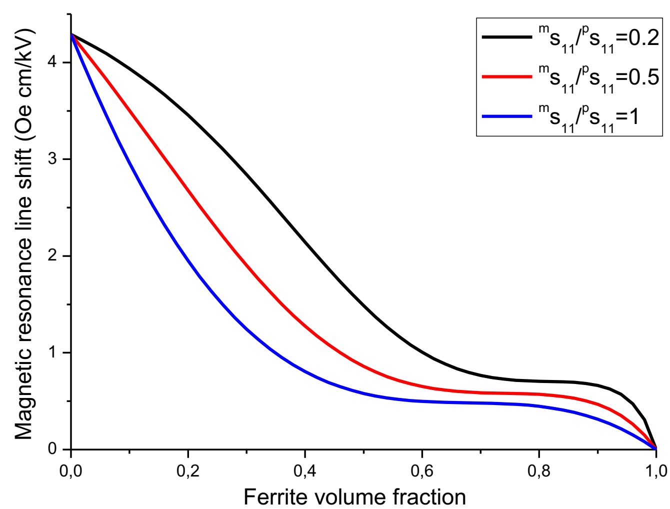

Fig. 11. Ferrite volume fraction dependence of magnetic resonance line shift at $E=1$ kV/cm for ferrite-piezoelectric bilayer for $\left|\frac{\lambda_{111}}{M_S}\right| = 0.16\cdot10^{-8}$ Oe^{-1}.

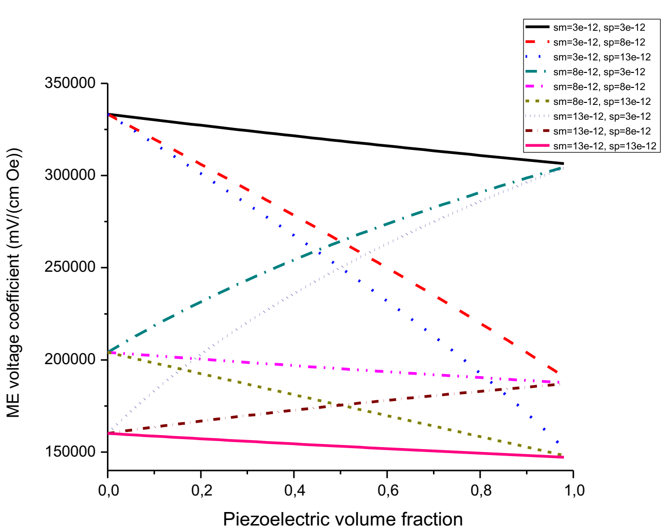

Fig. 9. EMR frequency versus piezoelectric volume fraction for longitudinal mode of 10 mm long magnetostrictive-piezoelectric layered structure.

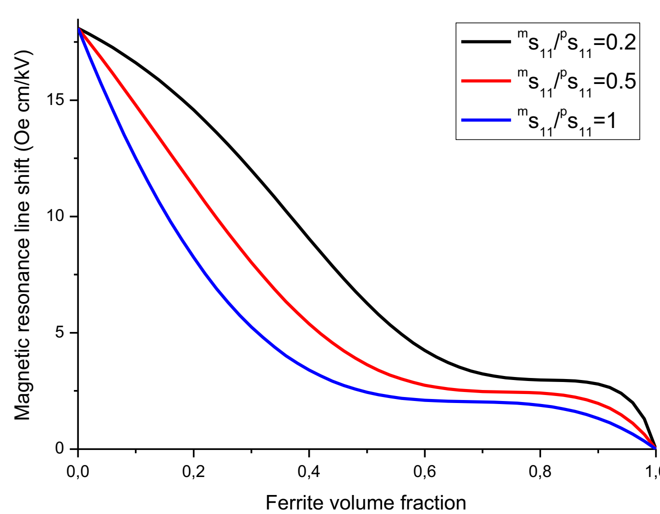

Fig. 12. Ferrite volume fraction dependence of magnetic resonance line shift at $E=1$ kV/cm for ferrite-piezoelectric bilayer for $\left|\frac{\lambda_{111}}{M_S}\right| = 0.68\cdot10^{-8}$ Oe^{-1}.

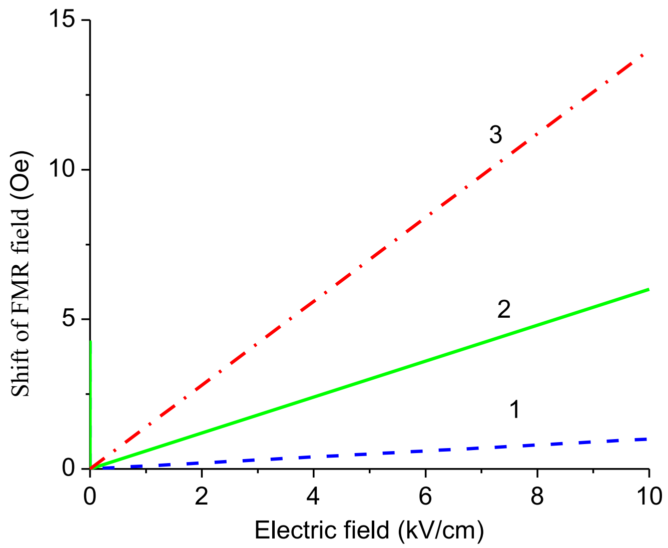

Fig. 13. Estimated shift of FMR field versus applied electric field at 9.3 GHz for the bilayers of YIG and PZT (1), NFO and PZT (2), and LFO and PZT (3) with equal thicknesses of magnetic and piezoelectric components.

volume fraction dependence of peak ME voltage coefficient at bending mode of magnetostrictive-piezoelectric bilayer is shown in Figs. 5 and 6 for different combinations of the piezoelectric and magnetostrictive layer compliances.

The bending resonance frequency is determined by expression $f_r = \frac{1.758}{\pi L^2}\sqrt{\frac{D}{^p\rho^p t + ^m\rho^m t}}$ and depends mainly on elastic compliances and volume fractions of initial components, and ratio $\frac{L}{\sqrt{t}}$. Piezoelectric volume fraction dependence of bending resonance frequency of magnetostrictive-piezoelectric bilayer is presented in Figs. 7 and 8 for different combinations of the piezoelectric and magnetostrictive layer compliances.

It should be noted that the resonance behavior of ME effect in a bilayer is dependent on end fixity conditions. We have limited ourselves by consideration of cantilever restraint since the giant ME interaction at lowest frequency possible is predicted for the bilayer fixed at one end and free at the other.

The resonance frequency is shown to increase with increasing bilayer thickness and decreasing length as in Figs. 7 and 8. The transverse ME voltage coefficient stands out above longitudinal due to the absence of demagnetization effect for the transverse case. The resonance frequency is characterized by a rather weak dependence on PZT volume fraction. This comes from nonlinear PZT volume fraction dependence of cylindrical stiffness of the sample.

4. Magnetoelectric coupling at axial mode of electromechanical resonance

Next we consider small-amplitude axial oscillations of the layered structures formed by magnetostrictive and piezoelectric phases. The displacement should obey the equation of media motion provided in Ref. [11]. To solve this equation, we used the boundary conditions for a bilayer that is free at both ends. Under assumption $^pK_{11}^2 << 1$, the fundamental EMR frequency is given by

$$f = \frac{1}{2L}\sqrt{\frac{^ps_{11} + r\,^ms_{11}}{^ps_{11}\,^ms_{11}(r\,^p\rho + ^m\rho)}}, \tag{5}$$

and the peak ME voltage coefficient at axial mode frequency is

$$\frac{\delta E_3}{\delta H_1} = \frac{8Q_a}{\pi^2}\frac{r\,^mq_{11}\,^pd_{31}/^p\varepsilon_{33}}{(r\,^ms_{11} + ^ps_{11})(r+1)}, \tag{6}$$

or $\frac{\alpha_E}{Q_a} = \frac{8}{\pi^2}\frac{V(1-V)\,^mq_{11}\,^pd_{31}/^p\varepsilon_{33}}{\left[V\,^ms_{11} + (1-V)\,^ps_{11}\right]}$

where Q_a is the quality factor for the EMR resonance.

It should be noted that Eqs. (5) and (6) for resonance frequency and ME voltage coefficient are valid for both bilayer and trilayer structures. It is easily seen from Eq. (6), that the piezoelectric volume fraction dependence of ME voltage coefficient divided by Q value is similar to that of low frequency ME coefficient (Eq. (2)). EMR frequency versus piezoelectric volume fraction is shown in Fig. 9.

The resonance enhancement of ME coupling is obvious from Eq. (6) and the ME coefficient at resonance is more than two orders of magnitude higher compared to low-frequency values. The coefficient $\alpha_{E,13}$ increases with increasing piezoelectric volume fraction, attains a peak value and then decreases with increasing V. Similarly to ME coupling in the low-frequency region, the theory predicts the highest ME coupling for in-plane fields (Fig. 10).

5. Magnetoelectric coupling in FMR region

For calculating the electric field induced shift of magnetic resonance line, we consider a bilayer of ferrite and piezoelectric. The ferrite component is supposed to be subjected to a bias field H_0 perpendicular its plane that is high enough to drive the ferrite to a saturated state. Next, we use the law of elasticity and constitutive equations for the ferrite and piezoelectric and the equation of motion of magnetization for ferrite phase.

The shift of magnetic resonance field can be expressed in the

Table 1
Material parameters for piezoelectric and magnetostrictive materials used for fabrication of layered structures.

Material	s_{11} (10^{-12} m^2/N)	s_{12} (10^{-12} m^2/N)	q_{33} (10^{-12} m/A)	q_{31} (10^{-12} m/A)	d_{31} (10^{-12} m/V)	d_{33} (10^{-12} m/V)	λ_{100} (10^{-6})	$\varepsilon_{33}/\varepsilon_0$
PZT	15.3	−5	–	–	−175	400	–	1750
BTO	7.3	−3.2	–	–	−78		–	1345
PMN-PT	23	−8.3	–	–	−600	1500		5000
Langasite	8.8	−4.3	–	–	$d_{14} = -3.65 \cdot 10^{-12}$ m/V	$d_{11} = 6.3 \cdot 10^{-12}$ m/V		50
Langatite	9.8	−3.8	–	–	$d_{14} = -2.81 \cdot 10^{-12}$ m/V	$d_{11} = 7.4 \cdot 10^{-12}$ m/V		77
Quartz	12.8	−1.8	–	–	$d_{14} = -0.67 \cdot 10^{-12}$ m/V	$d_{11} = 2.3 \cdot 10^{-12}$ m/V		4.68
YIG	6.5	−2.4			–	–	1.4	10
NFO	6.5	−2.4	−680	125	–	–	23	10
LFO	35	−12					46	10
Ni	20	−7	−4140	1200				
Terfenol-D	33.3	−10	15,707	4730	–	–		
Metglas	10	−3.2	14,000	−3000	–	–		

linear approximation in demagnetization factors due to electric field induced stress [13]:

$$\delta H_E = -\frac{M_0}{Q_1}[Q_2(N_{11}^E - N_{33}^E) + Q_3(N_{22}^E - N_{33}^E) - Q_4 N_{12}^E], \tag{7}$$

where

$$Q_1 = 2H_3 + M_0 \sum_{i \neq E} [(N_{11}^E - N_{33}^E) + (N_{22}^E - N_{33}^E)] ;$$

$$Q_2 = [H_3 + M_0 \sum_{i \neq E} (N_{22}^i - N_{33}^i)] ;$$

$$Q_3 = [H_3 + M_0 \sum_{i \neq E} (N_{11}^i - N_{33}^i)] ;$$

$$Q_4 = 2M_0 \sum_{i \neq E} N_{12}^i .$$

In Eq. (7), N_{kn}^i are effective demagnetization factors describing the magnetic crystalline anisotropy field ($i=a$), form anisotropy ($i=f$), field and electric field induced anisotropy ($i=E$).

As an example, we consider a specific case of magnetic field $\boldsymbol{H}$ along [111] axis. The shift of FMR field versus ferrite volume fraction is shown in Figs. 11 and 12. Electric field dependence of FMR field shift is presented in Fig. 13.

From the above results, we can conclude to obtain an optimum ME effect: (i) that the volume fraction of the piezoelectric phase should be high; (ii) that it is necessary to use a piezoelectric component phase with a large piezoelectric coefficient; and (iii) that it is necessary to use a magnetostrictive component phase with a small saturation magnetization and a high magnetostriction.

To obtain the estimates of ME coefficients from nomographs referred to above, one should use the material parameters of composite components. The relevant parameters of several materials that are most often used in ME structures are given in Table 1.

As an example of ME structure, we consider the bilayer of Ni and PZT with piezoelectric volume fraction 0.5. Based on data in Table 1, we get ${}^m s_{11} = 20 \cdot 10^{-12}$ m^2/N, ${}^p s_{11} = 15.3 \cdot 10^{-12}$ m^2/N, ${}^p d_{31} = -175 \cdot 10^{-12}$ m/V, ${}^m q_{11} = -4140 \cdot 10^{-12}$ m/A, ${}^p \varepsilon_{33}/\varepsilon_0 = 1750$. Fig. 4 at point A reveals the low-frequency ME voltage coefficient $\alpha_{E\ 31} = 190$ mV/(cm Oe). Then, Fig. 5 gives the peak ME voltage coefficient $\alpha_{E\ 31} = 20$ V/(cm Oe) at bending resonance frequency and Fig. 2 gives the peak ME voltage coefficient $\alpha_{E\ 31} = 70$ V/(cm Oe) at axial resonance frequency. Q-value is assumed to be equal to 100.

6. Conclusions

ME composites are known to enable the achievement of ME voltage coefficients many orders of magnitude larger than previously reported values for single phase materials. The advancements have opened up many possibilities in applications of sensors, transformers, and microwave devices. We presented here a new quick test of ME composites using nomographs and showed its use in applications where an approximate answer is appropriate and useful. To draw the graphs for ME voltage coefficients, we derived approximate expressions in explicit form for magnetically induced ME effect for different operational modes and laminate composite configurations including symmetrical and asymmetrical structures.

Another possible use of nomographs referred to above is predicting the volume fractions of composite components and sample geometry for specific composition to provide the strongest ME coupling.

In addition, a nomogram may be used to verify an estimate obtained from another exact calculation method notwithstanding the fact that the nomogram's accuracy is limited by the precision of reproducing the physical parameters.

Acknowledgment

The research was supported by a Grant from the Russian Science Foundation (Grant no: 15-19-10036).

References

[1] H. Schmid, A. Janner, H. Grimmer, J.-P. Rivera, Z. Ye. Proceedings of the 2nd International Conference on Magnetoelectnc Interaction Phenomena in Crystals, MEIPIC-2. Ferroelectrics, vol. 161–162, 1994.
[2] M.I. Bichurin, Proceedings of the 3rd International Conference on Magnetoelectric Interaction Phenomena in Crystals, MEIPIC-3. Ferroelectrics, vol. 204, 1997.
[3] J. Zhai, et al., J. Am. Ceram. Soc. 91 (2008) 351.
[4] S. Priya, et al., J. Electroceram. 19 (2007) 149.
[5] C.-W. Nan, M.I. Bichurin, S. Dong, D. Viehland, G. Srinivasan, J. Appl. Phys. 103 (2008) 031101.
[6] M.I. Bichurin, D. Viehland, Magnetoelectricity in Composites, Pan Stanford Publshing, 2012.
[7] G. Srinivasan, Annu. Rev. Mater. Res. 40 (2010) 153.
[8] C. Ederer, Nicola A. Spaldin, Nat. Mater. 3 (2004) 849.
[9] W. Eerenstein, N.D. Mathur, J.F. Scott, Nature 442 (2006) 759.
[10] R. Ramesh, Nicola A. Spaldin, Nat. Mater. 6 (2007) 21.
[11] M. Bichurin, V. Petrov, Modeling of Magnetoelectric Effects in Composites, Springer, 2014.
[12] M.I. Bichurin, V.M. Petrov, Adv. Condens. Matter Phys. 2012 (2012) 798310.
[13] M.I. Bichurin, V.M. Petrov, Ferroelectrics 162 (1994) 33.
[14] T.I. Muchenik, E.J. Barbero, Smart Mater. Struct. 24 (2015) 025039.
[15] H. Schmid, Ferroelectrics 162 (1994) 317.
[16] J. Van Suchtelen, Philips Res. Rep. 27 (1972) 28.
[17] J. van den Boomgaard, A.M.J.G. van Run, J. van Suchtelen, Ferroelectrics 14 (1976) 727.
[18] M.I. Bichurin, D. Viehland, G. Srinivasan, J. Electroceram. 19 (2007) 243.
[19] M.I. Bichurin, V.M. Petrov, S. Priya, In: Physical Effects, M. Lallart (ed.) (InTech., 2011), p. 277.